Observed relationships between the Southern Annular Mode and atmospheric carbon dioxide

Amy H. Butler,[1] David W. J. Thompson,[1] and Kevin R. Gurney[2]

Received 17 July 2006; revised 29 June 2007; accepted 16 August 2007; published 21 November 2007.

[1] The authors examine the observed relationships between large-scale climate variability and concentrations of atmospheric carbon dioxide (CO_2) in the Southern Hemisphere. The results reveal that month-to-month variations in the rate of change of atmospheric CO_2 at Palmer Station on the Antarctic Peninsula are significantly related to fluctuations in the dominant mode of Southern Hemisphere atmospheric variability, the so-called Southern Annular Mode (SAM). A similar but weaker relationship between the SAM and atmospheric CO_2 is evident at Syowa Station in eastern Antarctica, but not at the South Pole or stations located in Southern Hemisphere middle latitudes. Hence the SAM is most clearly related to fluctuations in atmospheric CO_2 at locations that sample the westerly flow over the high latitudes of the Southern Ocean. Results based on CO_2 flux estimates from the Atmospheric Tracer Transport Model Intercomparison Project (TransCom) suggest the observed relationships at least partially reflect the impact of the SAM on the flux of CO_2 over the Southern Ocean.

Citation: Butler, A. H., D. W. J. Thompson, and K. R. Gurney (2007), Observed relationships between the Southern Annular Mode and atmospheric carbon dioxide, *Global Biogeochem. Cycles*, *21*, GB4014, doi:10.1029/2006GB002796.

1. Introduction

[2] Numerous studies have examined the impacts on the carbon cycle of climate variability in the tropics and in the Northern Hemisphere, but relatively few studies have investigated the impacts on the carbon cycle of large-scale climate variability in the Southern Hemisphere.

[3] Most previous research on the relationships between climate variability and the carbon cycle is focused on the climate impacts of the El Niño–Southern Oscillation (ENSO) phenomenon. Previous studies have noted that atmospheric CO_2 decreases near the beginning of a warm ENSO event (El Niño) but increases as the ENSO event matures [*Bacastow*, 1976; *Keeling et al.*, 1989; *Elliot et al.*, 1991; *Conway et al.*, 1994]. The initial decrease in atmospheric CO_2 is thought to reflect a decrease in outgassing of CO_2 to the atmosphere as oceanic upwelling is reduced in the eastern tropical Pacific Ocean [*Feely et al.*, 1987, 1999]. The subsequent increase in atmospheric CO_2 is thought to reflect higher soil and plant respiration and an increase in forest fires associated with warmer temperatures and decreased precipitation over tropical land regions [*Keeling et al.*, 1989; *Van der Werf et al.*, 2004].

[4] More recent studies have examined analogous relationships between the carbon cycle and the Northern Hemisphere Annular Mode (NAM) [*Russell and Wallace*, 2004; *Schaefer et al.*, 2005]. The NAM is the dominant pattern of variability in the extratropical Northern Hemisphere (NH), and is characterized by out-of-phase fluctuations in the zonal wind between centers of action located at ~55–60°N and ~30–35°N [e.g., *Thompson and Wallace*, 2001]. *Russell and Wallace* [2004] demonstrated that winters corresponding to the high-index polarity of the NAM (defined as when the flow is anomalously westerly along ~55–60°N) are associated with increased drawdown of CO_2 into the terrestrial biosphere during the following spring. They reasoned the enhanced drawdown reflects the impact of the NAM on the extent of springtime snow cover and hence the length of the NH growing season. *Schaefer et al.* [2005] reached a similar conclusion on the basis of numerical experiments with a biosphere model.

[5] Here we examine for the first time analogous relationships between observations of atmospheric CO_2 and the Southern Annular Mode (SAM). Like its Northern Hemisphere counterpart, the SAM is characterized by out-of-phase fluctuations in the extratropical zonal wind, with centers of action located at ~60°S and ~40°S. However, in contrast to the NAM, the most pronounced climate impacts of the SAM are found not over land but over ocean regions. For example, during the high-index polarity of the SAM (defined as when the flow is anomalously westerly along ~60°S), sea surface temperatures (SSTs) are colder than normal throughout much of the high-latitude Southern Ocean but warmer than normal around 40°S [*Lovenduski and Gruber*, 2005; *Verdy et al.*, 2006; *Ciasto and Thompson*, 2007], and chlorophyll concentrations are on average lower than normal over the middle and high-latitude ocean areas of the Southern Hemisphere [*Lovenduski and Gruber*,

[1]Department of Atmospheric Science, Colorado State University, Fort Collins, Colorado, USA.
[2]Department of Earth and Atmospheric Sciences, Purdue University, West Lafayette, Indiana, USA.

0886-6236/07/2006GB002796$12.00

Table 1. Locations and Periods of Record for the Station Data Used in This Study

Station	Latitude	Longitude	Time Record	Location
Palmer Station (PSA)	64.92°S	64.00°W	1978–2004	Antarctica, barren seashore
Cape Grim (CGO)	40.68°S	144.68°E	1984–2004	Tasmania, cliff top
South Pole (SPO)	89.98°S	24.80°W	1975–2004	Antarctica, icy plateau
Halley Bay (HBA)	75.58°S	26.50°W	1983–2004	Antarctica, barren seashore
Syowa Station (SYO)	69.00°S	39.58°E	1986–2004	Antarctica, barren seashore

2005]. Model results suggest the high-index polarity of the SAM is also associated with changes in the ocean meridional overturning circulation, including increased upwelling of nutrient-rich waters in the region of ~60°S [*Hall and Visbeck*, 2002; *Sen Gupta and England*, 2006].

[6] The paper is organized as follows: In section 2 we discuss the data and methods. In section 3, we examine the relationships between the SAM and observations of atmospheric CO_2 concentrations over the high latitudes of the Southern Hemisphere. It is demonstrated that variations in the SAM are associated with statistically significant changes in the tendency of atmospheric CO_2 over the Antarctic Peninsula. Section 4 reviews the mechanisms whereby the SAM may impact atmospheric concentrations of CO_2 and examines results based on CO_2 flux estimates from the Atmospheric Tracer Transport Model Intercomparison Project (TransCom). Concluding remarks are provided in section 5.

2. Data and Methods

[7] Observations of atmospheric CO_2 are provided in monthly mean format by the Global Monitoring Division (GMD) at the National Atmospheric and Oceanic Administration (NOAA) [*Conway et al.*, 1994]. The GMD network consists of over 100 stations distributed globally. In this study, we focus only on stations that (1) lie over the middle and high latitudes of the Southern Hemisphere (i.e., regions where the climate impacts of the SAM are most pronounced) and (2) have at least 60% data coverage during the period 1980–2004. The stations used in the analysis are listed in Table 1. Note that some SH midlatitude stations in the GMD network have sparse data coverage are thus not included in the analysis (e.g., Tierra del Fuego and Crozet Island).

[8] Monthly mean geopotential height and wind data are derived from the National Centers for Environmental Prediction/National Center for Atmospheric Research reanalysis data set [*Kalnay et al.*, 1996; *Kistler et al.*, 2001], and were obtained through the NOAA Climate Diagnostics Center. The time series of the SAM is defined as the leading principal component time series of monthly mean 700 hPa height anomalies poleward of 20°S and was obtained from the NOAA Climate Prediction Center. Monthly mean values of the standardized SAM index used in this study are shown in gray in Figure 1, bottom.

2.1. TransCom Fluxes

[9] Monthly mean estimates of the interannual flux of CO_2 over the Southern Ocean are derived from the Atmospheric Tracer Transport Model Intercomparison Project level 2 simulations (TransCom: *Gurney et al.* [2002] and *Baker et al.* [2005]). The TransCom fluxes are estimates of the carbon exchange at the Earth's surface required to account for year-to-year variability in the observed concentrations of CO_2 measured at 23 stations located throughout the globe. The TransCom flux estimates are found as follows: (1) The world is discretized into 22 regions chosen on the basis of vegetation type (for land areas) and circulation features (for ocean areas); (2) an impulse unit flux is emitted separately from all 22 regions in thirteen different transport models; (3) the simulated CO_2 response is calculated as a function of lag and month at locations corresponding to the 23 well-sampled observing stations located throughout the globe (the combined response functions are referred to as the "TransCom response function matrix"); and (4) the model-specific TransCom response function matrices are inverted and projected onto the observed concentrations at the 23 observing stations for the period 1980 to 2002 via adjustment of the initial unit fluxes. In this study we are focused on the high latitudes of the Southern Hemisphere and thus use only (1) the inverse-derived fluxes over the Southern Ocean region and (2) the response functions for Antarctic stations to an impulse change in the flux of CO_2 over the Southern Ocean.

[10] Note that all of the transport models used in TransCom employed a single year of repeating transport winds (though not always the same repeating year) and hence there is no interannual variability in the atmospheric transport used in the models [*Gurney et al.*, 2002; *Baker et al.*, 2005]. However, year-to-year variability in CO_2 concentrations is thought to be dominated by variations in the flux rather than the transport of CO_2, particularly in the Southern Hemisphere [e.g., *Dargaville et al.*, 2000; *Rodenbeck et al.*, 2003; *Peylin et al.*, 2005]. Hence we expect the lack of interannual variability in the transport winds used in the TransCom models to have a minimal impact on the inverse-derived flux estimates used here. For more information on the TransCom methodology and the uncertainties of the flux estimates, see *Gurney et al.* [2002] and *Baker et al.* [2005].

2.2. Statistical Significance

[11] The statistical significance of all correlation coefficients is assessed using the *t* statistic. The effective sample size is estimated using the relationship outlined by *Bretherton et al.* [1999]:

$$N_{eff} \sim N^* \frac{1 - r_1 r_2}{1 + r_1 r_2} \tag{1}$$

where N_{eff} is the effective sample size; N is the sample size; and r_1 and r_2 are the lag-one autocorrelations of the time series being correlated. For example, in the case of

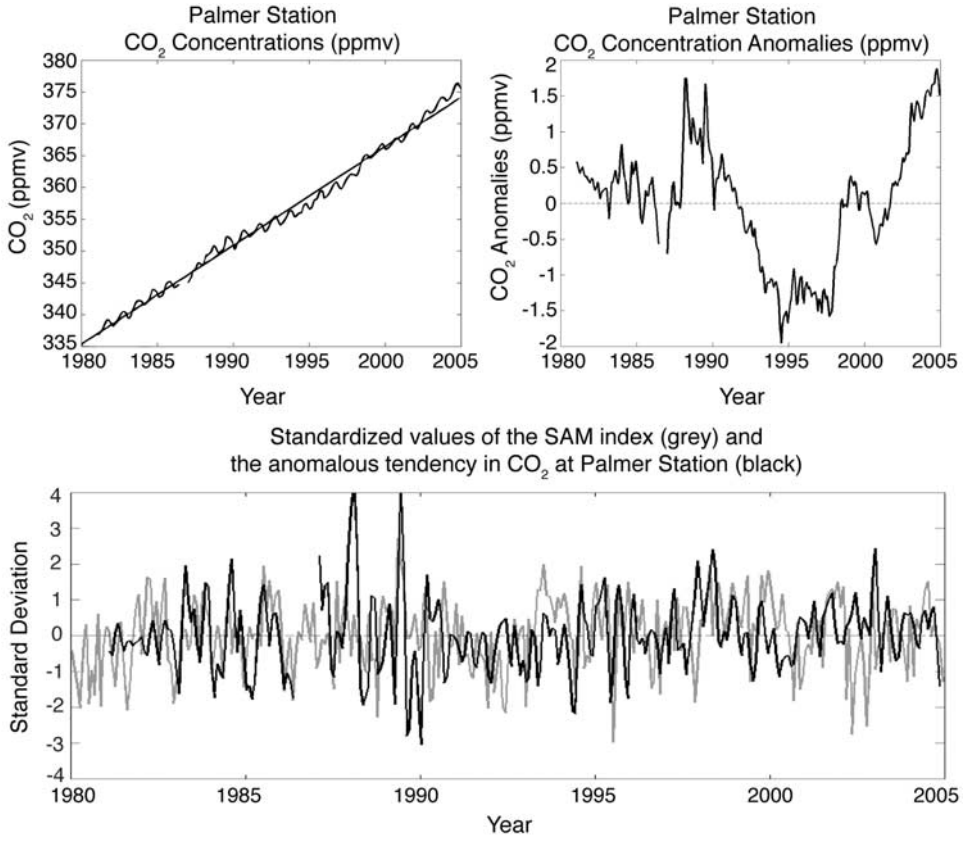

Figure 1. (top left) Time series of the concentration of CO_2 at Palmer Station. Linear fit to the curve is shown as the straight solid line. (top right) Time series of the anomalous concentration of CO_2 at Palmer Station, found by removing the linear trend and seasonal cycle from the time series in Figure 1, top left. (bottom) Standardized time series of the anomalous tendency in the concentrations of CO_2 at Palmer Station (black line), found by applying equation (2) to the time series in Figure 1, top left, and removing the seasonal cycle; and the standardized time series of the Southern Annular Mode (SAM) index (gray line).

correlations with CO_2 at Palmer Station (as investigated in the following section), the lag-one autocorrelation of the anomalous tendency time series is $r = 0.53$, the lag-one autocorrelation of the SAM time series is $r = 0.30$, and therefore the effective sample size for correlations between the two time series is $N_{eff} \sim 217$.

3. Analysis and Results

3.1. Comments on Analysis Design

[12] We investigate the relationships between the SAM and the observed tendencies in atmospheric CO_2 at the stations listed in Table 1. At all stations, the tendency in CO_2 at month t is defined as

$$\frac{d}{dt}(CO_2) = \frac{CO_2(t+1) - CO_2(t-1)}{2} \qquad (2)$$

where $\frac{d}{dt}(CO_2)$ is the change in CO_2 in units of ppmv month^{-1} and t is the time step (1 month). For example, the tendency in CO_2 for July 1983 is defined as $^1/_2$ times the difference between the concentrations for August 1983 and June 1983. We define tendencies as the difference across 2 months rather than consecutive months, since the latter definition yields a tendency time series lagged by half a month with respect to the concentration time series. Nevertheless, the results in the following section are not sensitive to the details of how the month-to-month tendencies are calculated. The seasonal cycle is removed to form anomalous tendency time series by subtracting the long-term climatological means from the tendency time series as a function of calendar month.

[13] We examine the tendencies in CO_2 rather than the concentrations in CO_2 for two reasons. First, we expect that month-to-month changes in the advection or flux of atmospheric CO_2 should be proportional not to the concentrations of atmospheric CO_2, but to the rate of change of CO_2. Similar reasoning has been exploited by *Bacastow* [1976] to examine the relationship between CO_2 and ENSO.

[14] Second, time series of atmospheric CO_2 have substantial memory and thus relatively few statistical degrees of

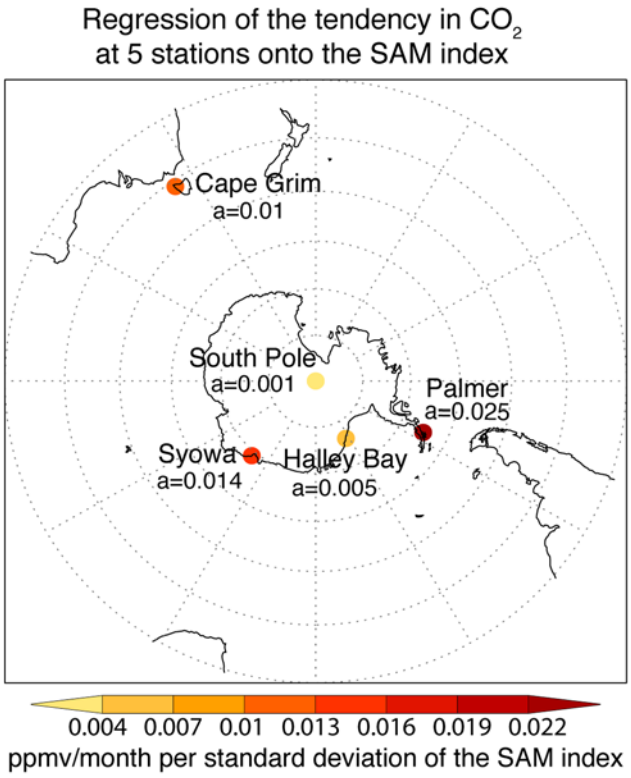

Figure 2. Regression of the tendency in CO_2 at the five stations listed in Table 1 onto standardized values of the SAM index. Shading is in units of ppmv month^{-1} per standard deviation of the SAM index. The only station with a corresponding correlation coefficient significant at the 2-tailed 95% level is Palmer Station.

freedom. For example, the time series of concentrations of atmospheric CO_2 from Palmer Station, Antarctica (Figure 1, top left) is dominated by the long-term trend and a comparatively weak seasonal cycle. If the linear trend of ~15 ppmv decade^{-1} and the seasonal cycle are removed from the data, the resulting time series (Figure 1, top right) is characterized by a relatively sparse number of low-frequency variations. The amplitude and timing of the low-frequency variations in the time series in Figure 1, top right, are sensitive to the manner in which the trend is removed from the data (i.e., whether via an exponential or linear fit). Thus correlations with time series of detrended concentration anomalies are based not only on few statistical degrees of freedom, but are also unstable to small changes in the analysis design.

[15] In contrast, the CO_2 tendency time series for Palmer Station as calculated in equation (2) (Figure 1, bottom, black line) has substantial variability from 1 month to the next and only a weak linear trend, which reflects the exponential growth of CO_2 over the past few decades. Hence equation (2) acts to diminish the amplitude of low-frequency variability relative to the amplitude of high-frequency variability in the time series of CO_2 concentrations. As noted in the previous section, correlations between the CO_2 tendency time series for Palmer Station (Figure 1, bottom, black line) and the SAM index (Figure 1, bottom, gray line) are based on ~217 effective degrees of freedom.

3.2. Regression Analysis

[16] Figure 2 shows the anomalous CO_2 tendency time series at the stations listed in Table 1 regressed onto standardized values of the SAM index time series. The most robust relationship between the SAM index and the tendencies in atmospheric CO_2 is found at Palmer Station on the Antarctic Peninsula, where CO_2 increases by 0.025 ppmv month^{-1} per standard deviation change in the SAM index. The corresponding correlation coefficient is significant at the 99% level on the basis of a 2-tailed test of the t statistic (t_{score} = 2.84). The second largest regression coefficient is found at Syowa, where CO_2 increases by 0.014 ppmv month^{-1} per standard deviation change in the SAM index. The associated correlation coefficient at Syowa is only significant at the 89% level on the basis of a 2-tailed test of the t statistic. Correlations for other stations are not statistically significant on the basis of the 2-tailed test of the t statistic (Figure 2).

[17] The small but highly significant correlation between the tendency in CO_2 at Palmer Station and the SAM index time series is tested further using the following Monte Carlo approach: (1) The CO_2 tendency and SAM index time series are randomly sorted by the order of years in the analysis (the sorting is done by year rather than months in order to preserve the autocorrelation characteristics of the original time series); (2) the regression coefficient between the sorted indices is calculated for 10,000 randomized sortings of the data; and (3) the regression coefficient of 0.025 ppmv month^{-1} from Figure 2 is compared with the histogram of the 10,000 regression coefficients on the basis of the randomized sortings of the data (Figure 3). As evidenced

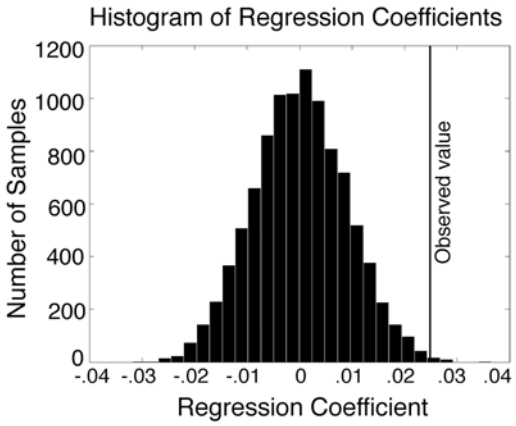

Figure 3. Histogram of regression coefficients found for 10,000 randomized sortings of the order of the years in the SAM index and anomalous CO_2 tendency time series at Palmer Station. Units are in ppmv month^{-1} per standard deviation of the SAM index. Observed regression value of 0.025 ppmv month^{-1} is denoted by the vertical line.

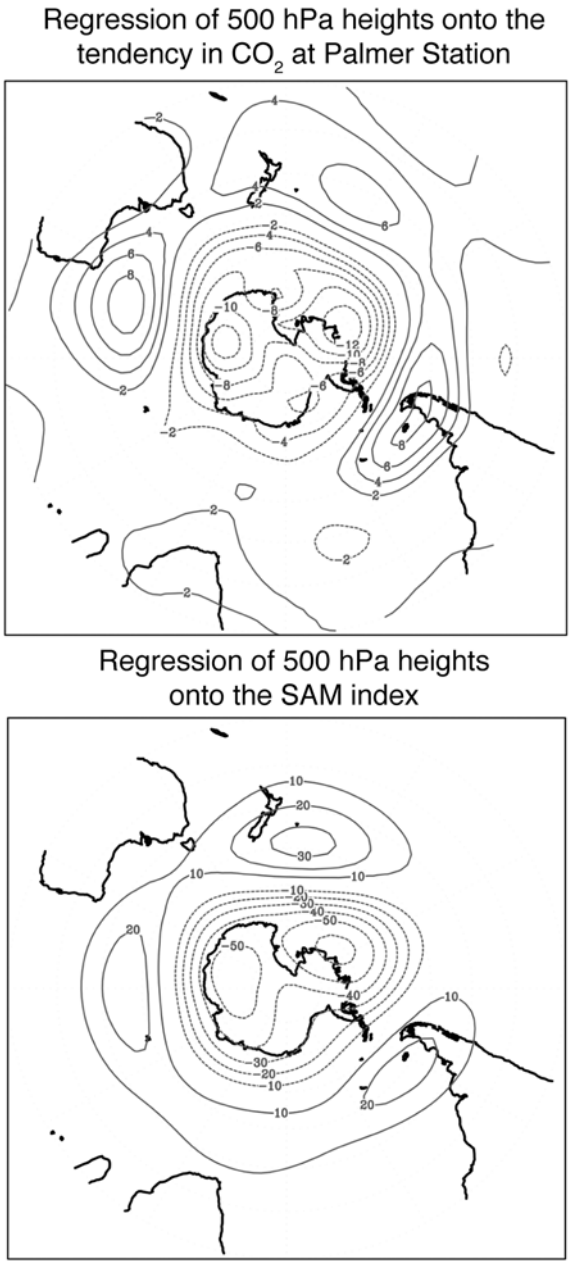

Figure 4. Regression of 500 hPa geopotential height anomalies onto (top) the time series of standardized anomalous CO_2 tendencies at Palmer Station for 1980–2003 and (bottom) standardized values of the SAM index for 1980–2003. Units are meters per standard deviation of the CO_2 tendency time series and SAM index, respectively. Note that the scale is different in the two panels.

in Figure 3, the regression coefficient from Figure 2 exceeds the regression coefficients for randomized sortings of the data in more than ~99.7% of the 10,000 sortings.

[18] The robustness of the relationship between the SAM and the anomalous tendency in CO_2 at Palmer Station is further explored in Figures 4–5. Figure 4 shows the patterns found by regressing 500 hPa geopotential height anomalies onto (top) standardized values of the anomalous tendency in CO_2 at Palmer Station and (bottom) standardized values of the SAM index. The results reveal that when CO_2 is increasing at Palmer Station, geopotential heights tend to be lower than normal south of ~60°S and higher than normal equatorward of 60°S. A comparison of the results in Figure 4, top, and Figure 4, bottom, reveals that the pattern of atmospheric circulation anomalies most closely related to the tendency in atmospheric CO_2 at Palmer Station (Figure 4, top) bears strong resemblance to the spatial structure of the SAM (Figure 4, bottom). Similar spatial patterns are obtained for regressions on the basis of geopotential height at all tropospheric levels.

[19] The relationship between the anomalous tendency in CO_2 at Palmer Station and the SAM peaks at a lag of zero months (Figure 5) and is not significant at any other lag. In fact, the rapid decay of the regression coefficients from their peak value at lag zero provides an additional sense of the robustness of the relationship between the SAM and CO_2 at Palmer Station. The linkage between the SAM and the tendency in CO_2 is stronger and more significant during the SH cold season (April–September) at both Syowa and Palmer Station (Table 2). Results for other stations are not significant during any season.

4. Possible Mechanisms

[20] What processes might give rise to the observed relationship between the SAM and the tendency in CO_2 over the Antarctic Peninsula? One possibility is that the SAM impacts the flux of CO_2 from the biosphere in the vicinity of Palmer Station. We view this explanation as

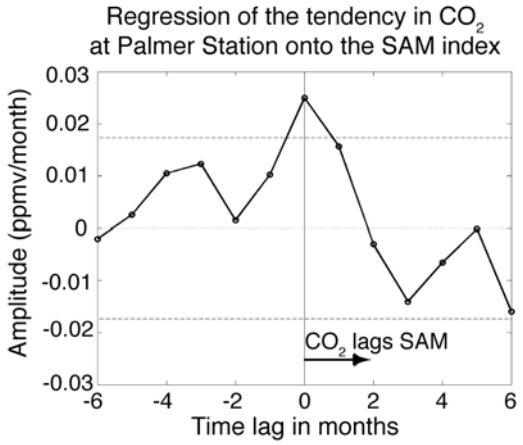

Figure 5. Lag regression of the anomalous tendency in CO_2 at Palmer Station onto standardized values of the SAM index. Positive lags indicate the tendency in CO_2 lags the SAM, and vice versa. Units are ppmv month^{-1} per standard deviation of the SAM. Dashed horizontal black lines denote the 95% significant levels based on a 2-tailed test of the *t* statistic.

Table 2. Regression Coefficients Between the Anomalous Tendencies in CO_2 at the Five Stations in Table 1 Onto Standardized Values of the SAM Index for the SH Cold (April–September) and Warm (October–March) Season Months[a]

Station Name	Regression Onto SAM, Cold Season	Regression Onto SAM, Warm Season	Regression Onto SAM, All Months
Palmer Station (PSA)	**0.032**	0.017	**0.025**
Cape Grim (CGO)	0.006	0.015	0.010
South Pole (SPO)	0.001	0.001	0.001
Halley Bay (HBA)	0.004	0.007	0.005
Syowa (SYO)	**0.021**	0.005	0.014

[a]Values that exceed the 2-tailed 95% confidence level are in bold font. Units are ppmv/month per standard deviation of the Southern Annular Mode (SAM) index.

unlikely, since Palmer Station lies on barren seashore, which is characterized by sparse vegetative coverage.

[21] A second possibility is that the anomalous winds associated with the SAM advect air from regions with different climatological mean levels of CO_2. For example, the vectors in Figure 6 show 925 hPa wind anomalies regressed onto standardized values of the anomalous tendency in CO_2 at Palmer Station (top) and the SAM index (bottom). As noted in the previous section and further exemplified in Figure 6, months with higher than normal tendencies in CO_2 at Palmer Station are associated with circulation anomalies that bear strong resemblance to the pattern of the SAM. Both the high-index polarity of the SAM and increasing CO_2 at Palmer Station are associated with 925 hPa wind anomalies that are predominantly westerly throughout the Southern Ocean, but have a weak northerly component at Palmer Station over the Peninsula.

[22] As evidenced in Figure 6, if the region to the northwest of Palmer Station is characterized by higher climatological mean levels of atmospheric CO_2 than the Antarctic Peninsula, then the anomalous flow associated with the high-index polarity of the SAM would bring anomalously high levels of CO_2 over Palmer Station. However, the horizontal gradients in climatological mean CO_2 are not well understood over the high-latitude Southern Ocean. In fact, published estimates suggest CO_2 increases slightly from the middle to high latitudes in the SH [e.g., *Tans et al.*, 1990], which is the opposite sign required to account for the relationships observed in Figure 2.

[23] A third possibility is that the SAM impacts the flux of CO_2 over the Southern Ocean, and that the resulting changes in atmospheric CO_2 are readily sampled at the Antarctic Peninsula because of the strong westerly flow in the Southern Hemisphere middle latitude atmosphere. Note that in contrast to the above mechanism, this explanation corresponds to advection by the atmospheric flow acting on anomalous, not climatological mean, gradients in CO_2.

[24] It is not possible from observations alone to prove that the SAM impacts the flux of CO_2 over the Southern Ocean. However, we can make inferences about the likelihood of this mechanism and also the amplitude of the required changes in flux using the inverse-derived flux estimates and response functions from the TransCom

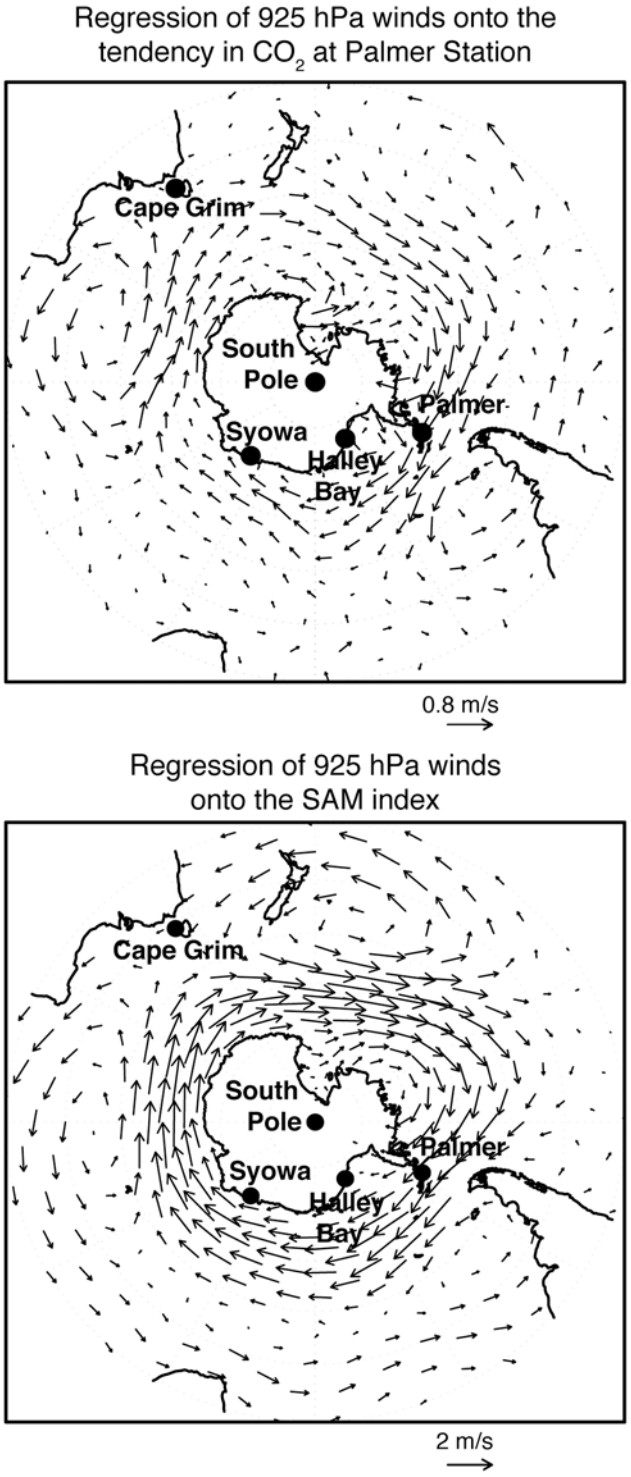

Figure 6. Regression of 925 hPa horizontal wind anomalies onto standardized values of (top) the anomalous CO_2 tendency at Palmer Station and (bottom) the SAM index, on the basis of data for 1982–2004. Vector units are meters/second per standard deviation of the basis time series. Note that the vector scale is different in the two panels.

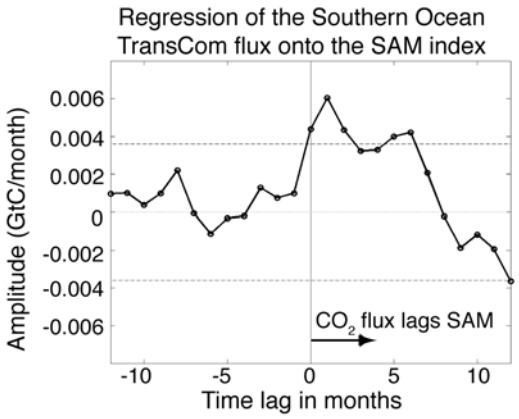

Figure 7. Lag regression of the time series of the TransCom Southern Ocean CO_2 flux estimates onto standardized values of the SAM index. Positive lags indicate the estimated CO_2 fluxes lag the SAM index, and vice versa. Units are GtC month^{-1} per standard deviation of the SAM index. Dashed horizontal lines denote the 95% significant levels based on a 2-tailed test of the *t* statistic. Results are based on data for 1980–2002.

experiment. Figure 7 shows the lag regression of the inverse-derived Southern Ocean CO_2 flux anomalies from the TransCom experiment onto standardized values of the SAM index using monthly mean data from 1980–2002. The SAM is only weakly related to the flux of CO_2 at lags preceding peak amplitude in the SAM index (which makes physical sense), and is most significantly correlated with the inverse-derived Southern Ocean fluxes at lags of 0 to 2 months. The timing of the SAM signature in the inverse-derived fluxes (Figure 7) differs slightly from the timing of the SAM signature in the observed concentrations at Palmer Station (Figure 5), but the sign of the fluxes and the concentrations are consistent: Both imply a net flux of CO_2 from the ocean to the atmosphere. The amplitude of the anomalous inverse-derived fluxes is ~0.005 GtC per month per standard deviation of the SAM index at lag zero.

[25] The physical consistency of the results based on the inverse-derived fluxes and the observed concentrations can be further explored using the TransCom "response functions." Recall from section 2 that the Southern Ocean "response functions" are the transport model responses at all observing locations to an impulse flux of CO_2 from the Southern Ocean region. Table 3 shows the annual mean response functions averaged over all TransCom transport models at Palmer Station, Syowa, and the South Pole to an impulse flux from the Southern Ocean of ~0.005 GtC (i.e., the amplitude of the inverse-derived flux in Figure 7). The response functions are in monthly resolution, and the results in Table 3 correspond to the net tendency during the first month after the flux anomaly. Both the amplitude and spatial structure of the responses are broadly consistent with the observed tendencies in Figures 2 and 5: The impulse flux gives rise to a change in concentration at Palmer Station of ~0.027 ppmv but weaker changes at Syowa and the South Pole. The spatial distribution of the results in Figure 2 and Table 3 suggests changes in CO_2 over the Southern Ocean are more readily apparent over the Antarctic Peninsula than at other Antarctic locations.

5. Concluding Remarks

[26] The results in Figures 2–5 reveal that variations in the SAM are associated with statistically significant changes in the tendency of atmospheric CO_2 over the Antarctic Peninsula. It is possible the results reflect anomalous mixing by the SAM of relatively high levels of climatological mean CO_2 from lower latitudes. However, at least 2 factors suggest the anomalous observed tendencies reflect the impact of the SAM on the flux of CO_2 over the Southern Ocean:

[27] 1. Results based on inverse-derived fluxes yield significant relationships between the SAM and the flux of CO_2 over the Southern Ocean (Figure 7). The associated transport model response functions are also consistent with the amplitudes and pattern of the observed anomalous tendencies: The largest response to an impulse flux of CO_2 from the Southern Ocean is found over the Antarctic Peninsula while weaker responses are found at Syowa and the South Pole (Table 3).

[28] 2. Recent numerical experiments run with a coupled physical-biogeochemical-ecological model simulate analogous changes in the flux of CO_2 over the Southern Ocean in response to changes in the SAM [*Lovenduski et al.*, 2007]. In fact, the amplitude of the simulated fluxes from this coupled model is virtually identical to the amplitude of the inverse-derived fluxes revealed here, given the same time and space constraints for fluxes from the Southern Ocean (N. Lovenduski, personal communication, 2007).

[29] The findings in this study thus provide observational support for possible feedbacks between the carbon cycle and large-scale climate variability in the Southern Hemisphere. Virtually all climate change simulations suggest that increased atmospheric CO_2 will lead to a poleward shift in the Southern Hemisphere storm track consistent with the high-index polarity of the SAM [*Kushner et al.*, 2001; *Miller et al.*, 2006], and there is now both modeling [*Lovenduski et al.*, 2007] and observational (this study) evidence that the high-index polarity of the SAM, in turn, drives anomalous fluxes of CO_2 from the high-latitude Southern Ocean to the atmosphere. *Toggweiler et al.* [2006] have suggested such a feedback may have been key in driving past climate changes. What such a feedback portends for the climate response to anthropogenic emission of CO_2 remains to be determined.

Table 3. TransCom Transport Model Responses at Palmer Station, Syowa Station, and the South Pole for a 0.005 GtC Per Month Flux From the TransCom Southern Ocean Region

Station Name	Concentration Response, ppmv
Palmer Station	0.027
Syowa Station	0.011
South Pole	0.007

[30] **Acknowledgments.** The research was funded in part by an AMS graduate fellowship, the United States Environmental Protection Agency (EPA) under the Science to Achieve Results (STAR) graduate fellowship program, and NASA grant NNG04GH53G. We thank N. S. Lovenduski and N. Gruber for helpful comments on the manuscript. We also thank the TransCom level 2 modelers and the NOAA Global Monitoring Division for providing the data sets.

References

Bacastow, R. B. (1976), Modulation of atmospheric carbon dioxide by the southern oscillation, *Nature*, *261*, 116–118.

Baker, D. F., et al. (2005), TransCom 3 inversion intercomparison: Impact of transport model errors on the interannual variability of regional CO_2 fluxes, 1988–2003, *Global Biogeochem. Cycles*, *20*, GB1002, doi:10.1029/2004GB002439.

Bretherton, C. S., M. Widmann, V. P. Dymnikov, J. M. Wallace, and I. Blade (1999), The effective number of spatial degrees of freedom of a time-varying field, *J. Clim.*, *12*, 1990–2009.

Ciasto, L. M., and D. W. J. Thompson (2007), Observations of large-scale ocean-atmosphere interaction in the Southern Hemisphere, *J. Clim.*, in press.

Conway, T. J., P. P. Tans, L. S. Waterman, and K. W. Thoning (1994), Evidence for interannual variability of the carbon cycle from the National Oceanic and Atmospheric Administration/Climate Monitoring and Diagnostics Laboratory Global Air Sampling Network, *J. Geophys. Res.*, *99*, 22,831–22,855.

Dargaville, R. J., R. M. Law, and F. Pribac (2000), Implications of interannual variability in atmospheric circulation on modeled CO_2 concentrations and source estimates, *Global Biogeochem. Cycles*, *14*, 931–943.

Elliot, W. P., J. K. Angell, and K. W. Thoning (1991), Relation of atmospheric CO_2 to tropical sea and air temperatures and precipitation, *Tellus, Ser. B*, *43*, 144–155.

Feely, R. A., R. H. Gammon, B. A. Taft, P. E. Pullen, L. S. Waterman, T. J. Conway, J. F. Gendron, and D. P. Wisegarver (1987), Distribution of chemical tracers in eastern equatorial Pacific during and after the 1982–1983 El Niño/Southern Oscillation Event, *J. Geophys. Res.*, *92*, 6545–6558.

Feely, R. A., R. Wanninkhof, T. Takahashi, and P. Tans (1999), Influence of El Niño on the equatorial Pacific contribution to atmospheric CO_2 accumulation, *Nature*, *398*, 597–601.

Gurney, K. R., et al. (2002), Towards robust regional estimates of CO_2 sources and sinks using atmospheric transport models, *Nature*, *415*, 626–630.

Hall, A., and M. Visbeck (2002), Synchronous variability in the Southern Hemisphere atmosphere, sea ice, and ocean resulting from the annular mode, *J. Clim.*, *15*, 3043–3057.

Kalnay, E., et al. (1996), The NCEP/NCAR 40-Year Reanalysis Project, *Bull. Am. Meteorol. Soc.*, *77*, 437–471.

Keeling, C. D., R. B. Bacastow, A. F. Carter, S. C. Piper, T. P. Whorf, M. Heimann, W. G. Mook, and H. Roeloffzen (1989), A three-dimensional model of atmospheric CO_2 transport based on observed winds: 1. Analysis of observational data, in *Aspects of Climate Variability in the Pacific and the Western Americas*, *Geophys. Monogr. Ser.*, vol. 55, edited by D. H. Peterson, 363 pp., AGU, Washington, D. C.

Kistler, R., et al. (2001), The NCEP-NCAR 50-year reanalysis: Monthly means CD-ROM and documentation, *Bull. Am. Meteorol. Soc.*, *82*, 247–268.

Kushner, P. J., I. M. Held, and T. L. Delworth (2001), Southern Hemisphere atmospheric circulation response to global warming, *J. Clim.*, *14*, 2238–2249.

Lovenduski, N. S., and N. Gruber (2005), The impact of the Southern Annular Mode on Southern Ocean circulation and biology, *Geophys. Res. Lett.*, *32*, L11603, doi:10.1029/2005GL022727.

Lovenduski, N. S., N. Gruber, S. C. Doney, and I. D. Lima (2007), Enhanced CO_2 outgassing in the Southern Ocean from a positive phase of the Southern Annular Mode, *Global Biogeochem. Cycles*, *21*, GB2026, doi:10.1029/2006GB002900.

Miller, R. L., G. A. Schmidt, and D. T. Shindell (2006), Forced annular variations in the 20th century Intergovernmental Panel on Climate Change Fourth Assessment report models, *J. Geophys. Res.*, *111*, D18101, doi:10.1029/2005JD006323.

Peylin, P., P. Bousquet, C. Le Quéré, S. Sitch, P. Friedlingstein, G. McKinley, N. Gruber, P. Rayner, and P. Ciais (2005), Multiple constraints on regional CO_2 flux variations over land and oceans, *Global Biogeochem. Cycles*, *19*, GB1011, doi:10.1029/2003GB002214.

Rodenbeck, C., S. Houweling, M. Gloor, and M. Heimann (2003), Time-dependent atmospheric CO_2 inversions based on interannually varying tracer transport, *Tellus, Ser. B*, *55*, 488–497.

Russell, J. L., and J. M. Wallace (2004), Annual carbon dioxide drawdown and the Northern Annular Mode, *Global Biogeochem. Cycles*, *18*, GB1012, doi:10.1029/2003GB002044.

Schaefer, K., A. S. Denning, and O. Leonard (2005), The winter Arctic Oscillation, the timing of spring, and carbon fluxes in the Northern Hemisphere, *Global Biogeochem. Cycles*, *19*, GB3017, doi:10.1029/2004GB002336.

Sen Gupta, A., and M. H. England (2006), Coupled ocean-atmosphere-ice response to variations in the Southern Annular Mode, *J. Clim.*, *19*, 4457–4486.

Tans, P. P., I. Y. Fung, and T. Takahashi (1990), Observational constraints on the global atmospheric CO_2 budget, *Science*, *247*, 1431–1438.

Thompson, D. W. J., and J. M. Wallace (2001), Regional climate impacts of the Northern Hemisphere Annular Mode, *Science*, *293*, 85–89.

Toggweiler, J. R., J. L. Russell, and S. R. Carson (2006), Midlatitude westerlies, atmospheric CO_2, and climate change during the ice ages, *Paleoceanography*, *21*, PA2005, doi:10.1029/2005PA001154.

Van der Werf, G. R., J. T. Randerson, G. J. Collatz, L. Giglio, P. S. Kasibhatla, A. F. Arellano Jr., S. C. Olsen, and E. S. Kasischke (2004), Continental-scale partitioning of fire emissions during the 1997 to 2001 El Niño/La Niña period, *Science*, *303*, 73–76.

Verdy, A., J. Marshall, and A. Czaja (2006), Sea surface temperature variability along the path of the Antarctic Circumpolar Current, *J. Phys. Oceanogr.*, *36*, 1317–1331.

A. H. Butler and D. W. J. Thompson, Department of Atmospheric Science, Colorado State University, 1371 Campus Delivery, Fort Collins, CO 80523, USA. (amy@atmos.colostate.edu)

K. R. Gurney, Department of Earth and Atmospheric Sciences, Purdue University, 550 Stadium Mall Drive, West Lafayette, IN 47907, USA.